An Honors Degree Project Presented for the
Partial Fulfillment of the
Degree of Bachelor of Science in
Neuroscience

Investigating the Role of the Annular Ligament in Zebrafish Cone Mosaic Formation and Maintenance

By
Corey Walsh

Undergraduate Program in Neuroscience
College of Literature, Science, and Arts
University of Michigan
Ann Arbor, Michigan
2015

Readers:

Dr. Pamela Raymond
Stephen S. Easter Collegiate Professor
MCDB Department

Dr. Richard Hume
Arthur F. Thurnau Professor
MCDB Director of Program in Neuroscience
MCDB Department

Dr. Kwoon Wong
Assistant Professor
MCDB Department

Investigating the Role of the Annular Ligament in Zebrafish Cone Mosaic Formation and Maintenance

Table of Contents:

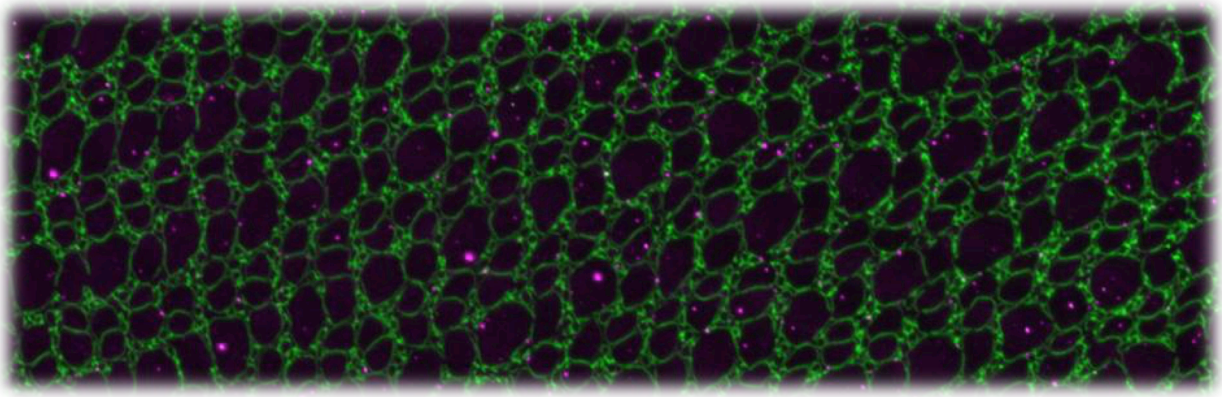

BACKGROUND:

Patterns in the Natural World:

Humans possess an uncanny ability to recognize patterns, which has largely defined human behavior since the dawn of the species. From providing key evolutionary adaptations allowing interpretive skills to granting opportunities for visual and auditory enjoyment through art and music, patterns and the facility to detect and identify them tightly link with the human experience. Nobel Laureate and economist Herbert Simon goes so far as to characterize human intuition as the capacity to subconsciously recognize patterns (Frantz, 2005), highlighting the implicit and explicit importance of pattern recognition to human nature. Collectively, patterns inherently fascinate us, which prompts a hunger to better understand how patterns form in the natural world and their functional importance. By gaining a better grasp on the subject, we can begin to unpack why these patterns consistently persist in nature, which may allow application in various fields of study.

The Teleost Cone Mosaic:

The zebrafish, *Danio rerio*, displays a uniquely precise cone photoreceptor mosaic pattern in the adult retina, a rare example of cell-fate and organization controlled at the single cell level (Salbreux et al., 2012). There persists, however, a lack of understanding of how and why these cone photoreceptors organize into such a pristine pattern. This thesis seeks to investigate the cone mosaic pattern. Zebrafish consistently prove to be ideal scientific models for exploration, particularly within the field of neuroscience. As shown previously, zebrafish serve as a genetic model in vertebrate regenerative studies, relying on abilities to regenerate fins, heart muscle, and nervous tissue after injuries (Win et al., 2009). Their lifelong growth also constitutes an

opportunity to study stem cells in vivo (Centanin et al., 2011). These key characteristics, along with many others, have enabled a large number of discoveries throughout the last few decades.

Zebrafish continue to fascinate researchers and provide an excellent model organism, specifically in retinal research. According to Walls, "the teleostean eye and retina, at their best, are outstanding in 'perfection' among all the fishes, and represent the fishes' nearest approach to the ocular quality of the very highest vertebrates" (Walls, 1942). The first recorded scientific work on the color vision of fish dates to 1884, with the subsequent millennium providing the groundwork for future experimentation on the visual system of fish (Walls, 1942). The early 1900s marked the understanding of cell morphology from histological sections of the teleost retina (Figure 1). This early research has largely contributed to the scientific community, garnering a deeper understanding of the vertebrate visual system that has set the stage for current research on the topic. For example, zebrafish retinal stem cells create the neural retina and pigment epithelium in a restricted, fate-specific manner, but these stem cells maintain multipotency, which may find applicability in tissue regeneration (Centanin et al., 2011). Radial Müller glia also retain multipotent retinal stem cell properties important for regenerative and developmental pathways, including cone photoreceptors (Bernardos et al., 2007). These studies serve as examples to better understand intrinsic factors that aid in determining photoreceptor cell fate choices. The precision of the cone mosaic patterning present in teleost fish, paired with the applicability and benefits of using zebrafish as a genetic animal model, may prove essential to discover key developmental processes that mediate cone photoreceptor cell-fate (Raymond & Barthel, 2004).

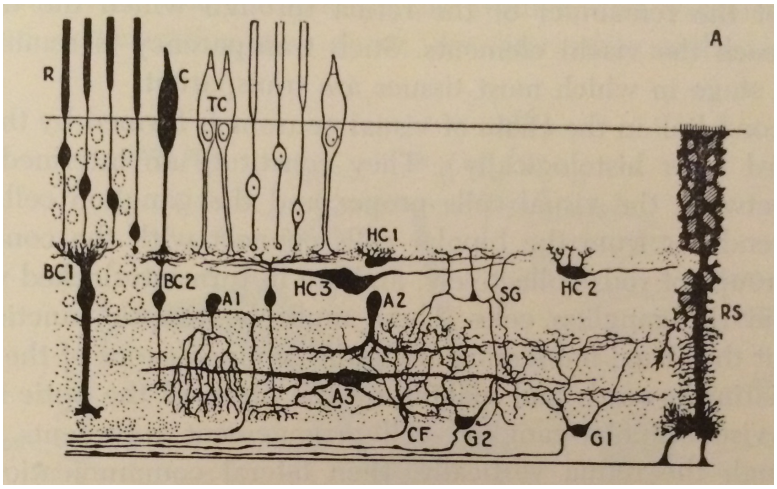

Figure 1. Vertical Section of the Teleost Retina. A 1-3, amacrine cells; BC 1-2, bipolar cells; C, cones; G 1-2 ganglion cells; HC 1-3 horizontal cells; R, rod; RS, radial supporting cell; SG, stellar ganglion cell; TC, twin cone (Brown, 1957).

In the zebrafish retina, cone photoreceptors organize in an intriguing mosaic pattern that perplexes researchers. During early development, the zebrafish retina displays a larval zone of cone photoreceptors without the characteristic mosaic. This patterning begins to form around three weeks post-fertilization (wpf), with alignment of cone columns forming at the germinal zone at the retinal periphery (Allison et al., 2011; Soules & Link, 2005). Shown schematically (Figure 2), the pattern involves alternating rows of blue and UV cone subtypes as well as red/green double cone subtypes, which are most sensitive to wavelengths of light after which they are named.

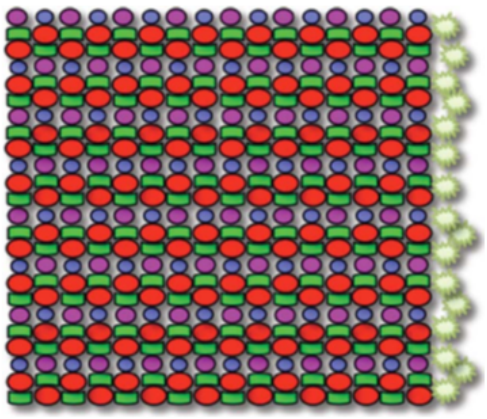

Figure 2. Cone Mosaic Schematic. Four cone photoreceptor subtypes organize in a precise pattern, with alternating rows of Blue/UV and Red/Green photoreceptor subtypes. Starbursts to the right represent proliferating cells in the marginal germinal zone, which forms circumferentially around the zebrafish retina (Allison et al., 2011).

Computational Modeling:

Previous research on the zebrafish retina involves collaborative efforts between the Department of Physics and Department of Molecular, Cellular, and Developmental Biology at the University of Michigan, using computational modeling to explain the formation of the cone photoreceptor mosaic. The model proposes that ordered columns of cells form due to the effects of planar cell polarity and anisotropic tissue-scale mechanical stresses (Salbreux et al., 2012). The hypothesis is partially supported by the planar-polarized distribution of Crumbs2a protein in differentiating cone photoreceptors near the retinal margin (Salbreux et al., 2012). The annular ligament may provide the mechanical stress proposed in this hypothesis, which leads to the hypothetical importance of the structure in this thesis.

The Annular Ligament:

The research projects described in this thesis investigate the mechanism behind cone mosaic formation and maintenance through utilizing selective genetic ablation techniques to target the annular ligament, a fibrous meshwork that runs circumferentially around the anterior of the zebrafish eye. Formation of the annular ligament has been reported to coincide with the appearance of the cone mosaic at about three wpf (Soules & Link, 2005), and we hypothesized that the annular ligament creates a circumferential, anisotropic stress that plays a key role in pattern formation and maintenance throughout the life of the zebrafish. The experiments reported here were also designed to better understand the dependency of cone mosaic formation on standard body size, time, or annular ligament development, primarily utilizing non-invasive imaging techniques throughout development.

The annular ligament forms a fibrous meshwork between the ciliary body and iris in teleost fish (Figure 3). Walls describes it as, “forming a bracket between cornea and iris, holding them

at a fixed angle to each other," which explains the origin of its name (Walls, 1942). The annular ligament forms at characteristic points in development, justifying the particular interest in the structure for this project. Embryonically, the annular ligament arises from mesodermal cells at the peripheral mesothelium of the cornea (Walls, 1942). It becomes visible by approximately 17 days post-fertilization (dpf) and greatly varies in shape between dorsal and ventral areas (Soules & Link, 2005). This progression of growth is shown in Figure 4. Globally, the structure forms a circumferential network proximal to the proliferative zone of retinal development.

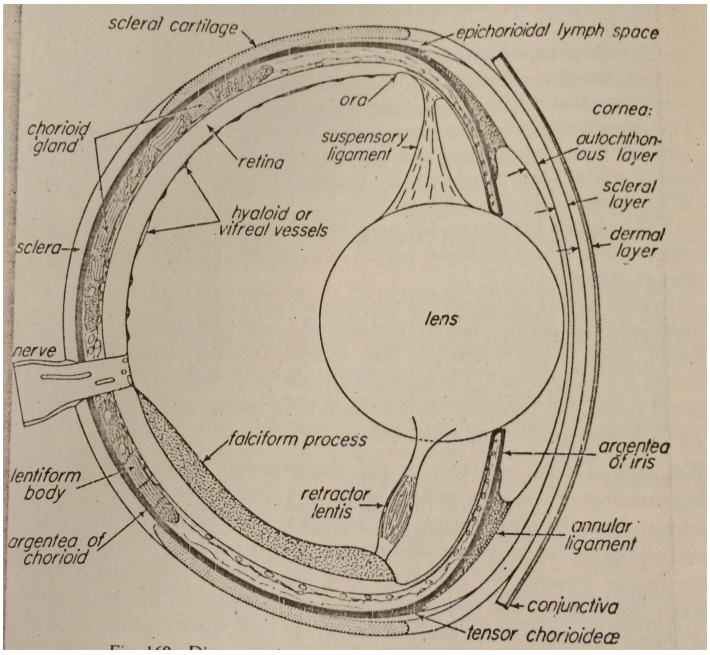

Figure 3. Teleost Eye Anatomy. Shows the relative location of the annular ligament within the zebrafish eye morphology. It forms a circumferential, fibrous network around the anterior eye (Walls, 1942).

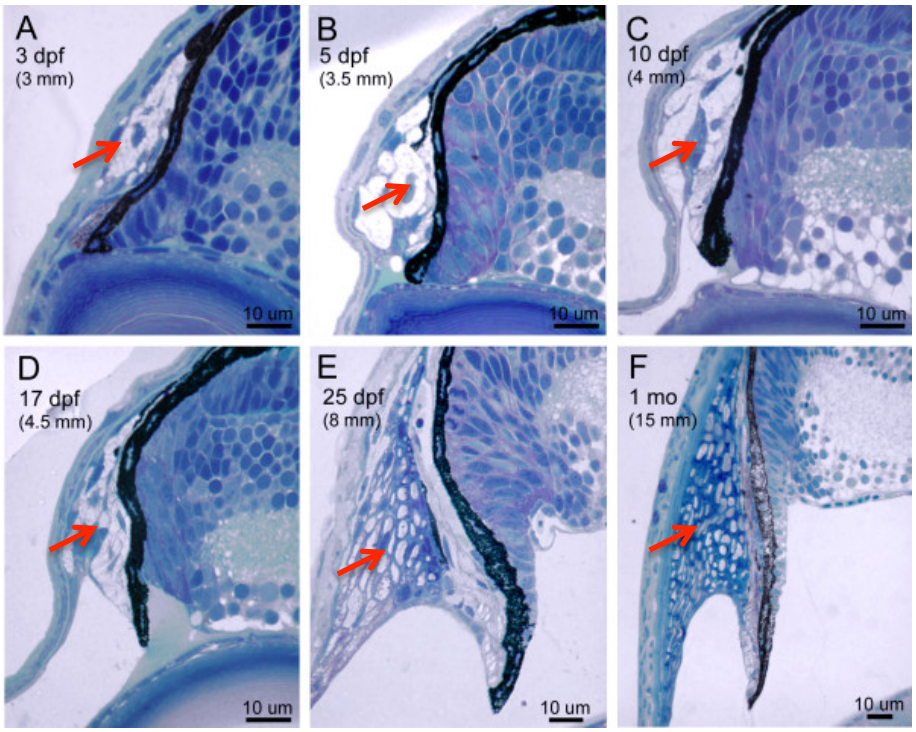

Figure 4. Morphogenesis of the dorsal iridocorneal angle. A) 3 dpf, **B)** 5 dpf, **C)** 10 dpf, **D)** 17 dpf, **E)** 25 dpf, **F)** 1mpf. Red arrows indicate developing annular ligament. Modified from (Salbreux et. al., 2012).

To date, no significant experimental data exists to explain the formation and maintenance of the zebrafish cone mosaic. One study proposes the spatiotemporal coordination of cell-cell interactions among cone progenitors to explain the identity and position of cone subtypes (Raymond & Barthel, 2004). This would suggest that signals from differentiating cones of specific subtypes mediate the fate of undifferentiated retinal progenitor cells (2004). Focusing on the fate of retinal progenitors, however, fails to fully take into account the orderly mosaic formation, which may be partially described by extrinsic factors stemming from zebrafish eye morphology. The annular ligament's proximity to the differentiating retinal progenitor cell layer makes it a notable suspect to investigate. We hypothesize that it provides anisotropic stress along the circumference of the proliferative zone to physically align cone photoreceptors into a lattice array.

Whereas intrinsic cues may provide information necessary to produce cone subtype identity, physical stress may contribute to the pristine columnar formation. With the appearance of the cone mosaic coinciding with the formation of the annular ligament at about three wpf (Salbreux et al., 2012), this may be a clear indication of the function of this fibrous network. Planar cell polarity within the epithelial sheets may also play a crucial role in modulating cell-cell adhesion (Salbreux et al., 2012). Together, both intrinsic and extrinsic cues likely induce the formation of the beautifully precise zebrafish cone mosaic.

Genetically Targeted Ablation of the Annular Ligament:

To conduct experimental analyses on the annular ligament requires a method to label the annular ligament in its entirety. We obtained a transgenic fish line to puruse this goal. Gelsolin protein is selectively expressed within the annular ligament, driving expression of a gelsolin-specific fluorescence reporter protein (Yoshikawa et al., 2007). This allows noticeable visualization of the annular ligament, which proves useful in the investigation of its form and function. The mCherry fluorescence protein shines red, outlining an annulus around the circumference of the eye (Figure 6A'). The mCherry reporter is a fusion protein carrying the bacterial enzyme nitroreductase, which allows for targeted, cell-specific ablation upon application of the prodrug metronidazole (Figure 5). The loss of mCherry fluorescence (Figures 6A", 6C) as well as a TUNEL assay (Figure 6D) confirmed the ablation of the annular ligament tissue following drug-treatment.

A past project by student Tiffany Anthony proved essential in providing baseline information for the methodology of subsequent projects. Initially, a transgene carrying gelsolin: nitroreductase-mCherry protein was embryonically introduced, and the resulting fish were selectively bred to form a colony of zebrafish carrying the desired transgene. At three wpf, a

subset of transgenic fish were treated with 5-ethynyl-2'-deoxyuridine (EdU) to visualize cells in the S-phase of mitosis. Subsequently, a group of these zebrafish underwent four consecutive nights of metronidazole treatment. At five wpf, the zebrafish underwent an additional EdU treatment to temporally notate the drug treatment within the growing cone mosaic. Retinas were dissected and analyzed using a flat-mount technique following a two to four month growth period after all drug treatments. Overall, this experiment confirmed the applicability of the nitroreductase-metronidazole mechanism for selective genetic ablation of the annular ligament.

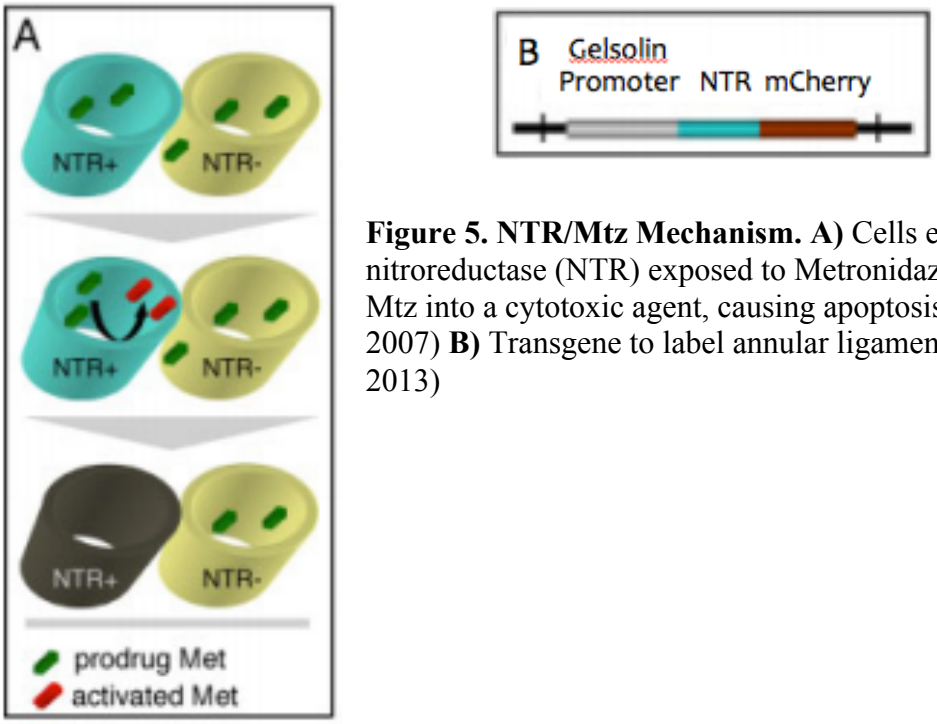

Figure 5. NTR/Mtz Mechanism. A) Cells expressing nitroreductase (NTR) exposed to Metronidazole (Mtz) convert Mtz into a cytotoxic agent, causing apoptosis, (Curado et al., 2007) **B)** Transgene to label annular ligament. (Tiffany Anthony, 2013)

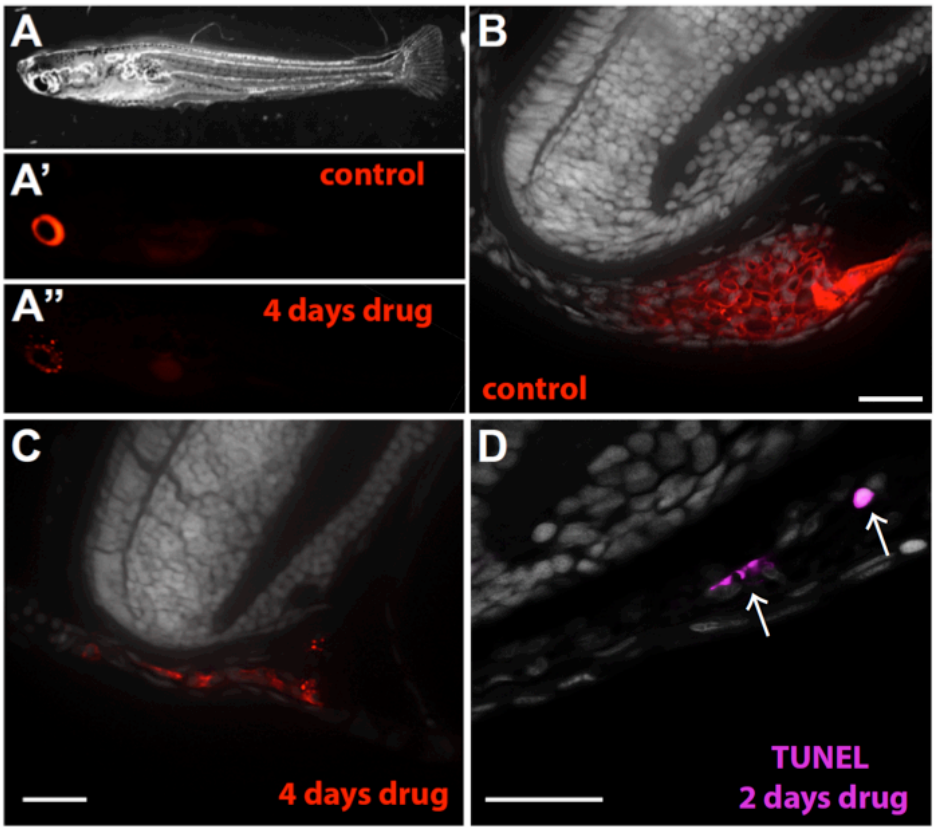

Figure 6. Annular Ligament Ablation. **A)** Wildtype zebrafish with no fluorescence, **A')** Control transgenic zebrafish with AL mCherry fluorescence, **A'')** Experimental zebrafish after 4 days of Mtz treatment **B)** Magnified view of A', **C)** Magnified view of A'', **D)** TUNEL staining indicating apoptosis. (Tiffany Anthony, 2013)

Learning from Tiffany Anthony's initial experiment, a number of modifications were introduced to subsequent experiments using the same general methodology of selective genetic ablation using the metronidazole-nitroreductase mechanism. To allow for more accurate visualization of the cone mosaic pattern, we crossed the fish carrying the gelsolin: nitroreductase-mCherry transgene with transgenic lines that label specific cone subtypes such as GFP labeled UV cones. We also investigated a longer, two-week metronidazole treatment period to create a more noticeable disruption of cone mosaic pattern formation. Lastly, a change in feeding protocol in the lab's standard operating procedures prompted quicker growth during larval and fry stages of development, ensuring that EdU labeling at four wpf took place well after the progression from larval to adult stages of retinal development.

EXPERIMENT ONE
MATERIALS AND METHODS:

Animals:

The zebrafish, *Danio rerio*, were obtained from a breeding colony of about 10,000 fish from the Raymond Lab at the University of Michigan. Zebrafish used in this experiment were used until 4-6 months post-fertilization (mpf). Fish were euthanized by submersion in aquatic anesthetic, tricaine (3-amino benzoic acidethylester).

Generation of Gelsolin-Promotor mCherry-Fluorescent Transgenic Animals:

In this project, I generated double transgenic zebrafish containing UV cone opsin reporter (sws1: GFP) and gelsolin: nitroreductase-mCherry transgenes using a cross between sws1: GFP parents and gelsolin: nitroreductase-mCherry parents. Progeny were screened at 4-12 dpf for GFP and mCherry fluorescence. F1 generations were used for experimentation and visualization of UV cone subtypes.

EdU Labeling and Detection of Mitotic Cells:

A 10 mM stock solution of EdU (Invitrogen cat #A10044) was prepared by dissolving 5 mg in 2 mL of dimethyl sulfoxide (DMSO). Stock solution was aliquot into 100 μL and stored at -20℃. 250 μL of 10 mM stock EdU solution was diluted with 20 mL fishwater for a 125 μM working solution. Fish were soaked for 2 hours at the end of 3 wpf and once again at the beginning of 6 wpf after drug treatment.

Metronidazole Treatment for Annular Ligament Ablation:

250 mL sterilized filter fish system water was added to 500 μL DMSO and mixed well. 125 mL was poured into a foil-covered flask, and 0.212 g metronidazole was added and mixed in the morning until fully dissolved by the afternoon. The remaining 125 mL DMSO solution was set aside for a control.

In the afternoon, 10-15 fish each were placed in the control and drug system water. To protect from light, the tanks were placed in a dark incubator with a bubbler. In the morning, the tanks were removed from the incubator, and the treatment water was replaced with filtered system water. Overnight treatment continued for a total of four repetitions for two weeks, using the weekends as resting periods due to fish intolerance of continuous metronidazole exposure.

Fixation of Isolated Adult Retinas:

At 4 mpf, fish were euthanized by anesthetic overdose. With Vannas micro-scissors and micro-tweezers, the optic nerve was severed, and the eye was removed from the body. A circumferential cut was made at the limbus, and the anterior segment was removed. The retina was flushed out of the eyecup using phosphate buffered saline. The retina was placed in fixative (4% paraformaldehyde in 0.1 M phosphate buffer, pH 7.4 with 5% sucrose), and short relaxing cuts were made along the perimeter of the retina. The tissue was immersion-fixed for 2 hours. After fixation, the tissue was rinsed three times for 15 each in 0.1 M phosphate buffer with 5% sucrose and then soaked in the same solution overnight.

EdU Click-iT Detection:

After isolation of adult retinas, whole mount Click-iT detection took place before immunohistochemistry detection. Isolated retinas were washed two times for 5 minutes each with 3% BSA in phosphate buffer solution (PBS), 1% Tween and 1% Triton. They were then washed for 20 minutes in PBS/1% Tween/1% Triton before a dark incubation period with agitation for 60 minutes in the Reaction Mixture. 555 Alexa Fluor secondary antibodies were used for sws1: GFP fish. After incubation, retinas were washed twice for 10 minutes in PBS/1% Tween/1% Triton.

Immunohistochemistry on Isolated Adult Retinas & Mounting:

Whole mount immunohistochemistry was carried out immediately after EdU Click-iT detection. Isolated retinas were blocked for 2 hours at room temperature with 10% normal goat serum, 1% Tween, and 1% Triton in PBS. Primary antibodies were diluted with 2% normal goat serum, 1% Tween, and 1% Triton in PBS and incubated overnight at room temperature. To label cone profiles, anti-ZO1 antibodies were used for GFP-fluorescent fish. After overnight incubation, the tissue was washed three times for 20 minutes each in PBS with 1% Tween, 1% Triton. Following the final wash, the tissues were mounted on a microscope slide and coverslipped under ProLong Gold.

Imaging & Processing:

Images were collected on a Zeiss Axio Image Z1 Epifluorescent Microscope (Carl Zeiss Microimaging Inc., Thornwood, NY). One global image at 2.5x magnification was taken initially, followed by images at 63x magnification with oil, using the Apotome Z-stack with a 0.3 μm step height at specified areas of the retina relative to a large ventral relaxation cut. These areas included the ventral-temporal, temporal-dorsal, dorsal, nasal-dorsal, and ventral-nasal regions. The 2.5x magnification global images were taken in between each region of high magnification, and enough high magnification images were taken to capture at least five columns of cone photoreceptors inside and outside the EdU labeled rings.

Adobe Photoshop CS5 Extended (Adobe Systems Inc., San Jose, CA) was used for processing of digital images gathered by the Zeiss microscope. Any digital adjustments to contrast or coloring were applied to the entire image, and Z-stacks were overlaid with multiple fluorescent channels.

RESULTS:

Image analyses of Tiffany's preliminary experiment yielded key background information to develop an improved procedure for subsequent projects, and it prompted new questions about the developmental time course of cone mosaic formation. Using a montaged, global image of one retina (Figure 7), a count of UV cones between the two rings of EdU-labeled cells gave an estimation of the number of circumferential cone columns produced per day during this stage of retinal development. These circumferential columns of cones are generated simultaneously and held together by planar polarized, cell-cell adhesion molecules present between adjacent cones within columns rather than across them (Salbreux et al., 2012). The rate of addition of new cones is approximately 4.42 columns per day temporally, 5.03 columns per day dorsally, and 4.358 columns per day nasally. Columnar tracings also led to procedural questions for systematically analyzing areas of suspected cone mosaic deformation (Figure 7). The analysis of the image highlighted difficulties in identifying areas to effectively and efficiently sample within a global image, posing serious time replication constraints. Furthermore, the disruption of primarily red-green double cones shown in Figure 7 prompts questions about differential effects of the drug treatments on varying cone photoreceptor subtypes. Altogether, these preliminary experiments proved essential in formulating a long-term framework for investigating zebrafish cone mosaic formation and maintenance.

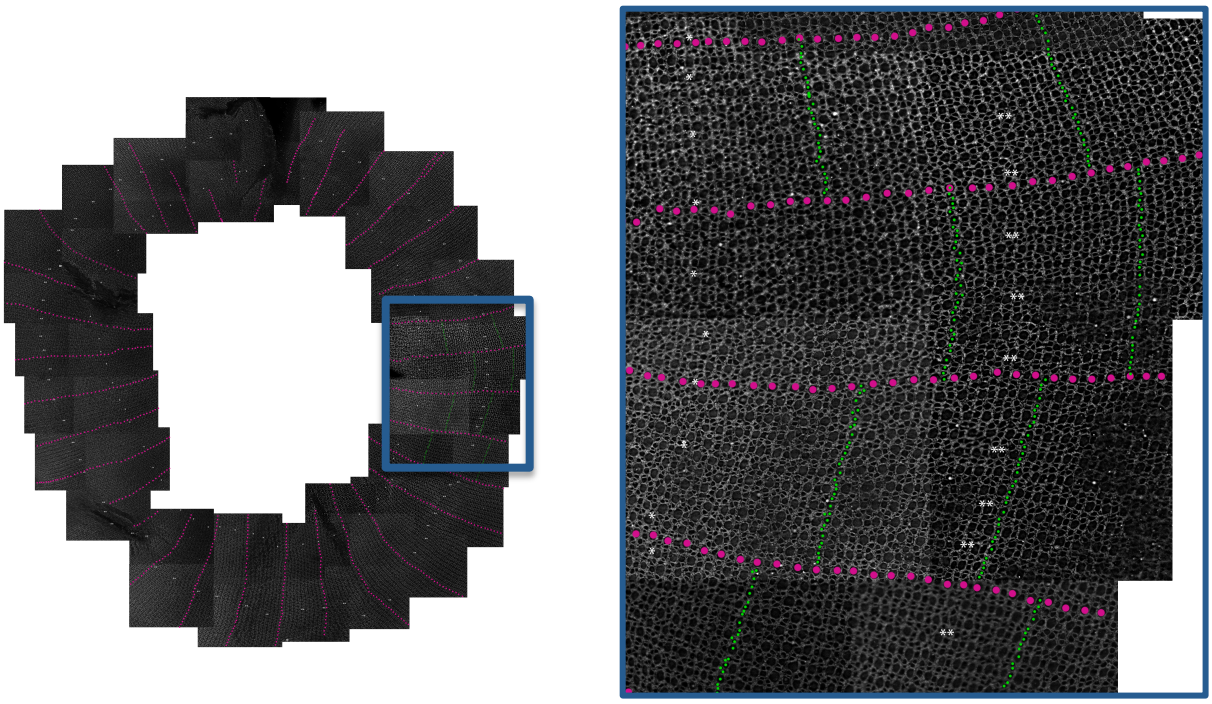

Figure 7. Global Retinal Image of Drug-treated Fish. Inner EdU labeling (green) corresponds to cones generated prior to drug treatment, and outer EdU labels to cones generated after drug treatment. Magenta labels rows of UV cones. (Modified from Mikiko Nagashima, 2013)

In experiments following Tiffany's, a variety of technical challenges limited the suitable number of samples for global retinal analysis. One of these samples can be seen in Figure 8, the right eye of a drug-treated fish. Inner and outer EdU labeled rings were marked and visible in temporal-dorsal, ventral-temporal, and ventral-nasal areas. No obvious pattern disruption was noted.

Subsequent imaging of drug-treated and control fish showed extensive growth of the retina after EdU labeling in fish that were not exposed to the metronidazole and reduced growth in the drug-treated fish (Figure 9). This would indicate the effects of the drugs toxicity upon the growth of the zebrafish, which here manifests as reduced growth.

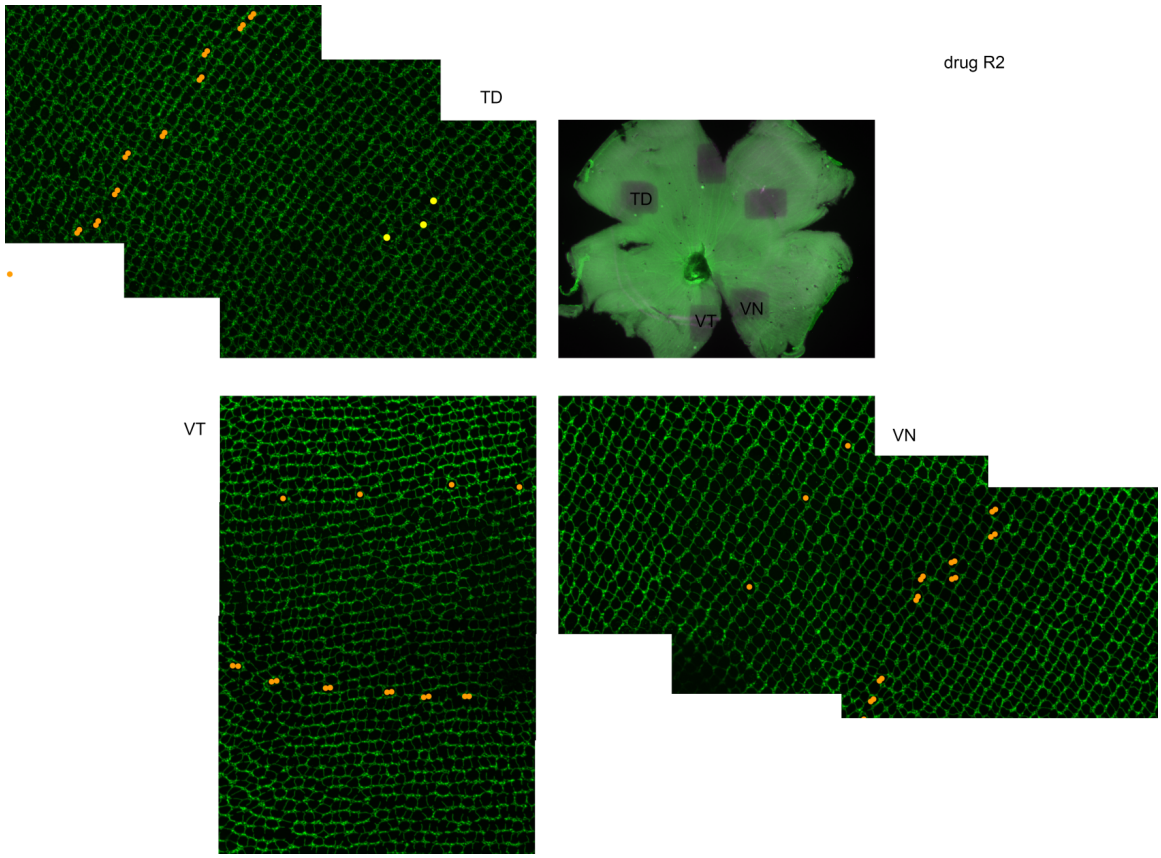

Figure 8. Right Retinal Image of Drug-Treated Fish. TD=temporal-dorsal, VT=ventral-temporal, VN=ventral-nasal regions of the eye. Single orange dots correspond to inner EdU rings, and double orange dots correspond to outer EdU rings. The area between these rings corresponds to the period of drug-treatment with metronidazole to selectively ablate the annular ligament.

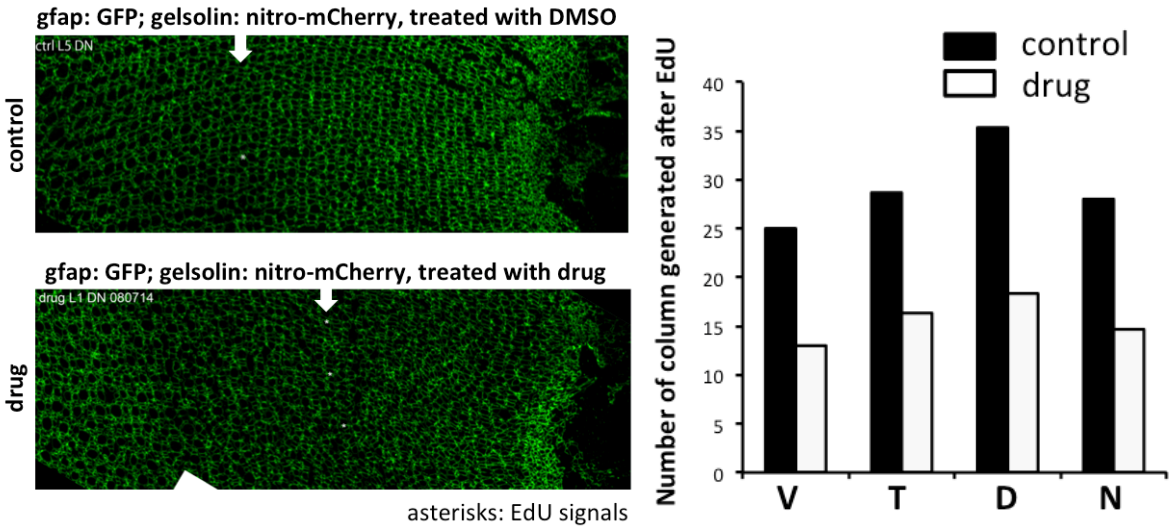

Figure 9. Columnar Generation of Drug-Treated and Control Fish. The left images show extensive growth after EdU labeling in control fish compared to drug-treated fish. The right image shows graphic representation of columnar generation differences. V=ventral, T=temporal, D=dorsal, and N=nasal regions. (Mikiko Nagashima, 2014)

DISCUSSION:

Experiment one proved to be incredibly time-intensive for the procurement of limited retinal images for analysis. We expected to observe a disruption in the cone mosaic pattern after annular ligament ablation. However, imaging showed minimal, if any, pattern disruption between the EdU labeled rings (Figure 8). These results fail to support the hypothesis that the annular ligament plays a role in organizing the cone mosaic. Alternatively, the lack of disruption may be due to the extended period of growth for 2-4 months that took place between the second EdU labeling and retinal isolation. This may have allowed ample time for columnar reorganization to take place following the regeneration of the annular ligament.

Another limitation within this experiment is the evidence of metronidazole toxicity (Figure 9). There was a clear lack of retinal growth in drug-treated fish following the second EdU labeling, which implies that there may be systemic effects in these drug-treated fish that impairs development following prolonged exposure to metronidazole.

Subsequent experimentation would benefit from the use of live-imaging techniques to enable the monitoring of cone mosaic patterning and annular ligament regeneration in vivo, which may provide a better understanding of a potential influence of the annular ligament relative to the cone mosaic formation in the zebrafish retina. Another methodological strategy would be to use laser ablation of the annular ligament rather than a drug-mediated, genetic ablation. This would mitigate the toxicity effects of the metronidazole while still allowing spatial and temporal selectivity in annular ligament ablation.

The completion of experiment one led to a considerable number of additional questions. Due to the toxicity of the metronidazole drug, the drug-treated zebrafish failed to develop at a typical rate, which led to questioning of the confounding effects of the toxic drug. This delay in

development extended to growth of the retina at the margin, which displayed a decrease in expected growth. Lastly, a lack of noticeable pattern disruption in the EdU labeled region of annular ligament ablation failed to support the initial hypothesis. Collectively, these results led to the creation of a follow-up experiment that questioned the dependency of cone mosaic formation on standard body size, time, or annular ligament development, primarily utilizing non-invasive imaging techniques throughout development.

Experiment two, on the other hand, provides context to questions we seek to answer concerning the reliance on the formation of the cone mosaic pattern upon key periods of zebrafish development measured through a variety of parameters. To date, most research links cone pattern formation as a time-dependent activity, with the mosaic appearing at about three wpf towards the end of larval development. This subsequent project involves live imaging of clear phenotype zebrafish with GFP fluorescent UV cone subtypes to estimate the formation of patterning within the developing retina. The clear phenotype proves crucial in allowing the live imaging of fish throughout development. Through a proxy measurement of annular ligament formation as well as a standardized assay of body length, we asked whether formation of the cone mosaic was correlated with age or size. The use of crowded and uncrowded environments led to a variety of fish sizes of the same age due to the release of growth-inhibiting pheromones in the crowded tanks (Francis et al., 1974).

EXPERIMENT TWO
MATERIALS AND METHODS:

Animals:

The zebrafish, *Danio rerio*, were obtained from a breeding colony of about 10,000 fish from the Raymond Lab at the University of Michigan. Zebrafish used in this experiment were used until 6-7 wpf. Fish were anesthetized via submersion in aquatic anesthetic, tricaine (3-amino benzoic acidethylester) prior to infliction of pain. This experiment used a dilution of the anesthetic to ensure revival for continued live imaging.

Zebrafish in both uncrowded and crowded conditions were placed into separate 4 L tanks and fed with approximately equal amount of food per fish. The number of fish in each tank was the only variable to lead to a variety of body sizes ($n_{uncrowded}$=10, $n_{crowded}$=50).

Generation of Clear Phenotype, Gelsolin-Promotor mCherry-Fluorescent Transgenic Animals:

Double transgenic zebrafish containing the sws1: GFP and gelsolin: nitroreductase-mCherry transgenes were crossed into fish with double recessive alleles for the pigmentation mutations *alb* and *roy*. The *alb* mutants lack melanin, and the *roy* mutants lack iridophores. This was done by crossing parents of genotypes *alb* -/-; *roy* -/- X sws1: GFP; gelsolin: nitroreductase-mCherry. This yielded an F1 generation of *alb* +/-; *roy* +/-; sws1: GFP; gelsolin: nitroreductase-mCherry, which were in-crossed to yield 16 potential genotypes in the F2 generation. These embryos were screened for a clear phenotype, followed by a screening of GFP and mCherry fluorescence at 4-12 dpf.

Total Body Length Measurement:

At 1 wpf, 2 wpf, 3 wpf, and 6 wpf, fish in crowded and uncrowded conditions were imaged using a Leica Light Microscope (Leica Microsystems, Bannockburn, IL 60015) at 2.5x,

2x, 1.25x, and 0.71x magnifications respectively. ImageJ was used in processing of these images to measure the tip-to-tip body length of zebrafish in a standardized manner. Ten fish from each condition were sampled, with those from the uncrowded condition chosen at random and those from the crowded condition from a selected range of fish sizes to ensure sampling of upper and lower bounds of the effects from the crowding factor. Fish were suspended in 3% methylcellulose to allow proper maneuvering for imaging.

Annular Ligament Assay:

At 1 wpf, 2 wpf, and 3 wpf, fish in crowded and uncrowded conditions were imaged using the Zeiss Axio Image ZI Epifluorescent Microscope (Carl Zeiss Microimaging Inc., Thornwood, NY) at 10x magnification. Through the use of a standardized threshold of mCherry intensity on ImageJ, the area of annular ligament was measured in μm^2. Fish were suspended in 3% methylcellulose to allow proper maneuvering for imaging of a global view of the annular ligament, with each fish resting on its side.

Pattern Formation Assay:

At 1 wpf, 2 wpf, and 3 wpf, fish in crowded and uncrowded conditions were imaged using the Zeiss microscope at 10x magnification. Fish were suspended in 3% methylcellulose to allow proper maneuvering for imaging of a dorsal view of the retina to ensure imaging of the proliferating marginal zone. Fish containing a minimum of three consecutive, linear rows of cones were considered to be patterned, or at least beginning to form a significant mosaic pattern.

Statistical Tools:

Using an alpha value of 0.05, an independent, unpaired t-test was run to determine the statistical significance of the difference between total body length measurements between crowded and uncrowded conditions. The same independent, unpaired t-test was conducted to

find the statistical significance of the difference between annular ligament saturation. Tests were run using Microsoft Excel 2011 (Microsoft Co., Redmond, WA).

RESULTS:

This experiment asked whether the formation of the zebrafish cone mosaic and annular ligament are dependent on either body size or age. Addressing this question required a sample of zebrafish of the same age but with variable body sizes. At 1 wpf, the mean total body length of uncrowded fish was 4.59 mm $\pm$ 0.17, while the mean total body length of crowded fish was 4.54 mm $\pm$ 0.32. Of these 1 wpf fish sampled, 40% showed signs of patterning, 13% showed no signs of patterning, and 47% of images were inconclusive (Figure 10).

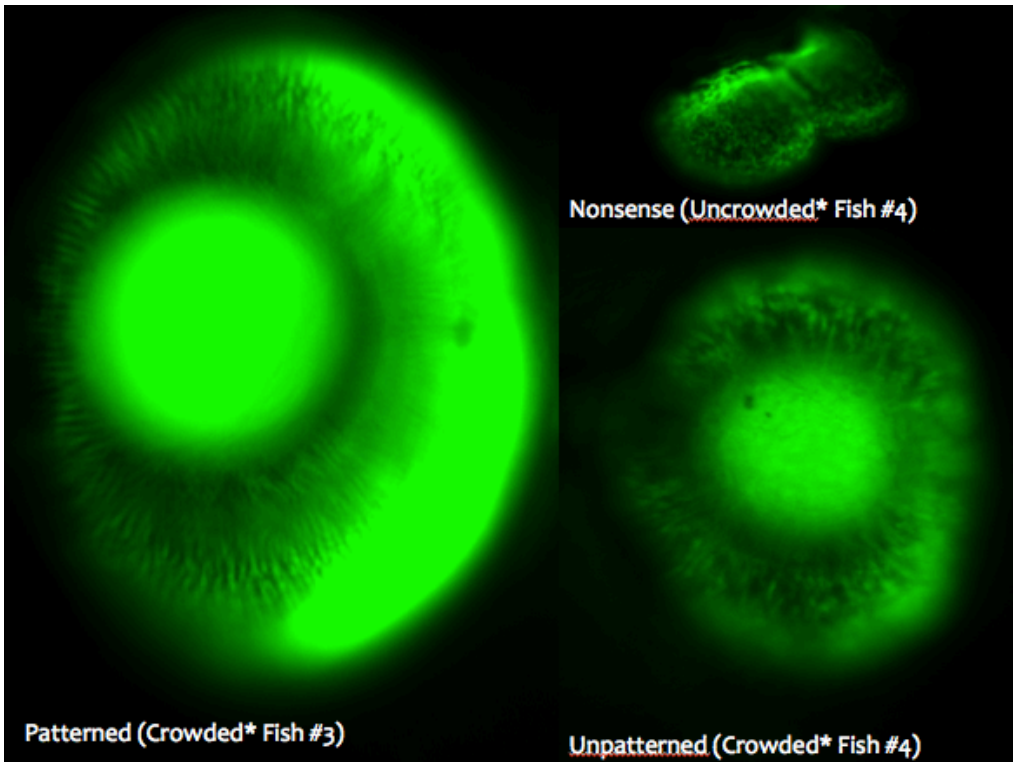

Figure 10. Patterning Classifications at 1 wpf. The left image shows clearly consecutive, linear rows of UV cones at the margin. The upper right image shows a fish that could not be properly imaged due to difficulties in maneuvering while anesthetized, and the lower right image shows an unpatterned retina at 1 wpf. *denotes that all fish, though separated into respective sampling groups, were not yet subject to crowded or uncrowded conditions.

After 1 wpf, zebrafish were first introduced to their crowded and uncrowded environments. Imaging and measurements took place at 2 wpf and showed an average mean of 6.11 mm $\pm$ 0.51 for uncrowded fish and 5.86 mm $\pm$ 0.54 for crowded fish. This difference was not statistically significant with an alpha value of 0.05. At this stage of development, however, 100% of fish sampled showed signs of patterning (Figure 11).

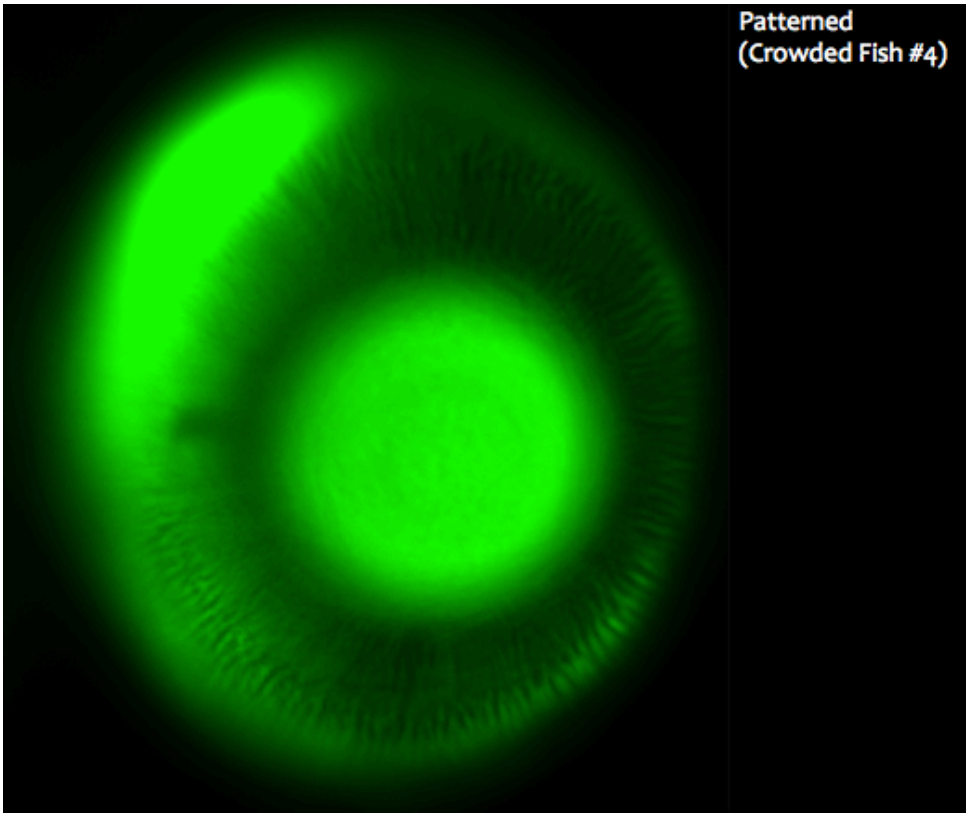

Figure 11. Pattern Formation at 2 wpf. This image shows clear formation of linear, consecutive rows of UV cones.

At 3 wpf, uncrowded fish had a mean total body length of 8.50 mm ± 0.45, while crowded fish had a mean total body length of 7.26 mm ± 0.82. This difference was statistically significant with a p-value of 0.0006. At this stage of development, 100% of sampled fish showed patterning, with the clearest view of the mosaic (Figure 12).

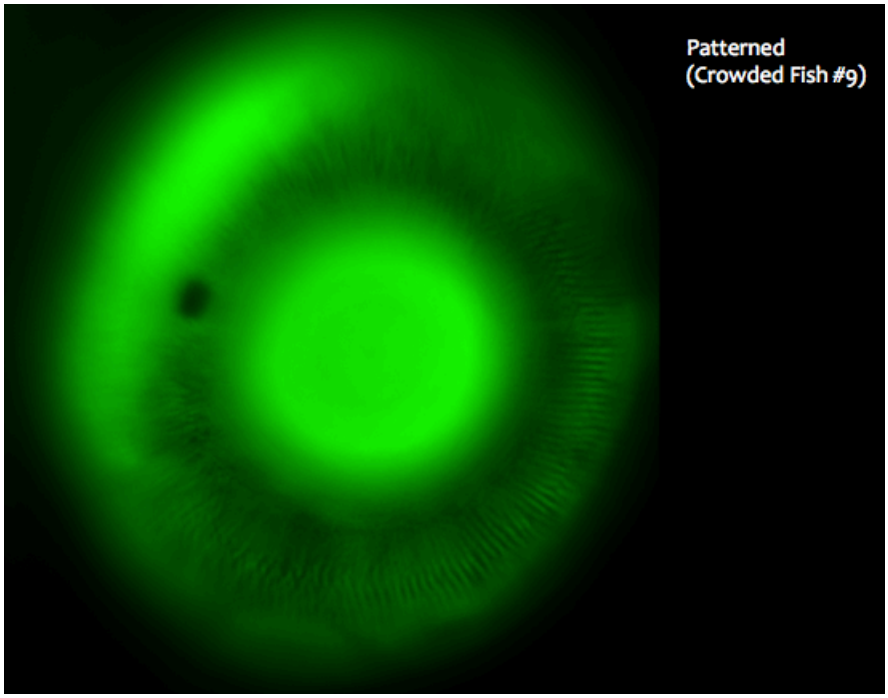

Figure 12. Pattern Formation at 3 wpf. The clearest view of the cone mosaic pattern through GFP fluorescent UV cone subtypes.

Body length measurements again took place at 6 wpf to confirm the effects of the crowding factor. The uncrowded sample mean was 16.05 mm ± 2.65, and the crowded sample mean was 12.42 mm ± 1.88. This difference was statistically significant with a p-value of 0.0015. Results of crowding can be seen graphically in Figure 12.

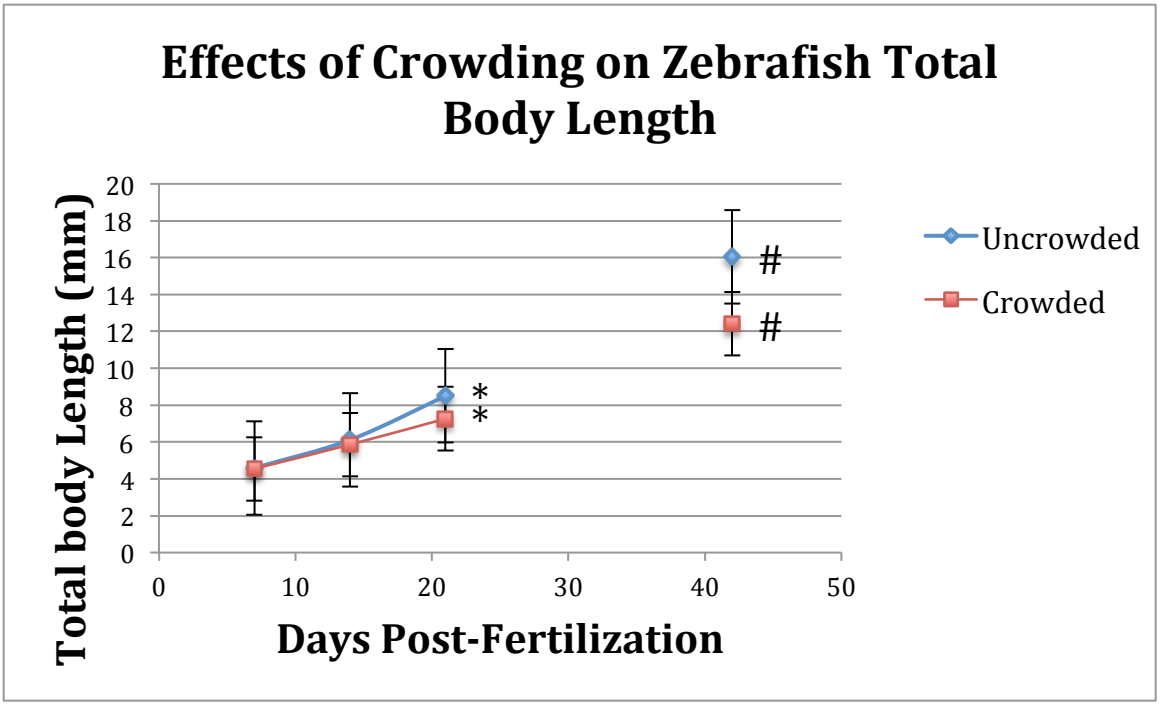

Figure 12. Effects of Crowding on Zebrafish Total Body Length. Graphical representation of divergence of total body length mean values between crowded an uncrowded zebrafish sample populations. *p=0.0006 #p=0.0015

Total surface area of the annular ligament visualized in living fish (Figure 14) showed a mean value of 10,528 $\mu m^2 \pm$ 2,780 for patterned fish at 1 wpf, and 11,093 $\mu m^2 \pm$ 882 for unpatterned fish at 1 wpf. Using an independent, unpaired t-test, these values proved not statistically significant. Patterned fish at 2 wpf had a mean annular ligament area of 21,550 $\mu m^2 \pm$ 5,454. As stated previously, there were no unpatterned fish at 2 wpf to sample.

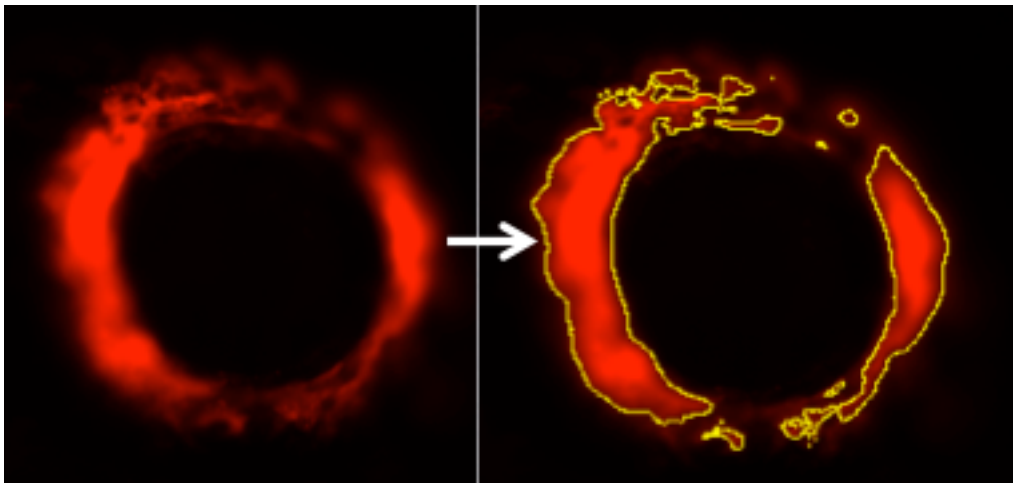

Figure 14. Annular Ligament Assay. Process used in ImageJ to measure the area of the annular ligament using a standardized threshold of color.

DISCUSSION:

Ultimately, this experiment led to more questions regarding the dependency of the cone mosaic pattern formation upon age, total body size, or annular ligament development. We were surprised to find evidence of cone mosaic formation as early as 1 wpf.

After being exposed to crowded conditions, zebrafish indeed showed signs of varying total body length, presumably in response to a crowding factor that has been studied in other teleost species (Yu & Perlmutter, 1970). Results at 3 wpf and 6 wpf were statistically significant using an independent, unpaired t-test. Despite abundant food, these species-specific crowding factors work to inhibit the growth of some individuals (Yu & Perlmutter, 1970). The growth inhibiting effects appear most significant in juveniles, and may be accelerated from the effects of excessive exposure to metabolic wastes like ammonia (Yu & Perlmutter, 1970). Crowding factors also depress heart rates, which may lead to other complications during development (Francis et al., 1974). Fish do, however, show different thresholds of responsiveness to the crowding factor when exposed to varying concentrations (Francis et al., 1974). Measurements of crowding factor concentration can be made in subsequent experimentation using trichloroethane as an extraction tool (Pfuderer et al., 1974).

Aside from potential confounding effects of the growth inhibition from the crowding factor, which was part of the experimental procedure, a number of other concerns arise about the interpretation of collected data. In analyzing the annular ligament, it proved difficult to use a standardized exposure setting that would properly visualize the annular ligament formation in all sampled zebrafish. As a result, some of the intensity of mCherry may be variable between sampled retinas, potentially hindering the usefulness of this measurement data.

The quality and shape of the annular ligament fluorescence also calls into question the viability of this measurement tool in the clear phenotype zebrafish. *Roy* mutants still maintain small amounts of shiny pigmentation within the body, and some of the fluorescence found while imaging may be a result from light reflections from iridiphores in the iris. This would lead to a seemingly brighter intensity of apparent mCherry fluorescence from the pigment cells rather than the mCherry protein. This may be alleviated in the future by using immunocytochemistry to quantitatively separate mCherry protein as an assay for annular ligament development.

The benefits of live imaging on the Zeiss microscope lie in the ability to monitor the development of the cone mosaic pattern in vivo over the span of weeks. This also enables the opportunity to show organizational changes that may occur months after fertilization, though this was not pursued in this particular experiment. The use of clear phenotype zebrafish for live imaging also eliminates the lengthy process of retinal dissection and isolation. Additionally, excessive handling and exposure to chemicals may damage the retina after the work put into isolation.

Overall, imaging techniques on the Zeiss microscope proved less than satisfactory. This may be in part due to the difficulty in orienting young fish in the methylcellulose gel. There are, however, alternatives that may prove more useful in subsequent experimentation. The use of the Z-stack technique used in experiment one might prove more useful in accurately imaging the formation of the cone mosaic and annular ligament in vivo. The use of a confocal laser microscope may also be more effective, though more costly.

Further, the use of the tip-to-tip total body length as a measurement tool for body size measurements should be amended in future experimentation. Rather than measuring from the tip of the nose to the tip of the tail, measuring from the tip of the nose to the base of the tail would

have mitigated confounding effects of varying tail lengths of the developing zebrafish. This experiment would have benefited from this standard body length measurement.

Lastly, image analysis leads to broader questioning of what the definition of a patterned retina should be. In this experiment, three consecutive linear rows were used as an arbitrary definition of patterning, but this definition may not be robust. This experiment indicated that the change from unpatterned to patterned cone mosaic may in fact be gradual during early developmental stages.

Experimentation in this thesis showed the ability of zebrafish to regenerate columnar organization of the cone mosaic pattern following damage to proximal structures within the eye and clarified limitations with drug-mediated genetic ablation of the annular ligament. It also revealed pattern formation as early as 1 wpf, which challenges previous understanding of the time course for generation of the cone mosaic. Although much remains unclear about the relationship between the annular ligament and the cone mosaic, experiments one and two shed light on cone mosaic formation and maintenance in the developing zebrafish. It is likely that both intrinsic and extrinsic cues mediate the formation of this crystalline pattern, and subsequent research must be completed to reach a resolution on the subject.

AFTERWORD:

This afterword uses the word queer when appropriate. This deliberate choice means to reclaim ownership of a word often used in hate speech to define, limit, and ridicule the human experiences of many who fail to fit the mold of a heteronormative, oppressive society. It is used to highlight a collective separation from these systems of power and privilege, to symbolize independence and self-definition, and to empower the LGBTQA-Z community at large.

The scientific community breeds excellence. By rewarding merit, intelligence, and unbiased investigation, it harnesses the powerful minds of individuals posing questions to explain the natural world. This system, however, does not come without flaws. Research communities often create high-pressure environments valuing a meritocracy devoid of effective heterogeneity, which stifles the formation of supportive communities engaged in conversations of social justice and diversity.

That scientific research consistently produces applicable results is a misconception by society at-large, which threatens to shake the foundation of scientific integrity. Years of research on a particular topic may yield minimal publications or relevant conclusions, which may negatively affect the psyche of those engaged in scientific inquiry. Anecdotes of misguided scientific judgment and fabricated data haunt the histories of many high-achieving academic institutions. The formation of resilient communities that rely on supportive attitudes, however, may mitigate these negative effects upon the psyche. By creating a diverse scientific community, a shift in thought can be made to value those who may fail to conform to a normative society. This conscious shift promotes happy, healthy communities that engage in a variety of ways to approach situations based upon the vastly different lived experiences they may hold.

Accurately, van Anders describes how “we are often actually actively discouraged from thinking about issues like empowerment or social justice, because science tells us through instruction and/or immersion that these are ideological concerns that have no place in (ideologically-neutral) science” (2012). This type of separation from ideological issues

effectively describes how the scientific community self-personifies as a machine of unbiased, pure thought: a dangerously flawed concept of reality. A focus on neutrality, precision, and perfection sets up the scientific community for long-term failure, and a collective upheaval of systemic thought may usher in a more productive environment that values pathos as well as logos.

In order to consciously derail from systemic, homogenous thought, the identities upon which we grow and build our sense of individuality must be taken into active consideration. Though we may all be scientists, it proves increasingly crucial to consider how this identity may intersect with other identities we may hold. This theoretical framework aids in understanding how individuals occupy many identities, which may cross at many different avenues (Crenshaw, 1991). Stated astutely, "the problem with identity politics is not that it fails to transcend difference, as some critics charge, but rather the opposite – that it frequently conflates or ignores intragroup differences" (Crenshaw, 1991). Intersectionality would indicate that the lived experiences of a white, Muslim individual from Ann Arbor, MI may differ from that of a Muslim person of color from Turkey. While the two individuals may both identify as Muslim, the intersection of their other identifies both racial and geographic may lead to vastly different experiences throughout their life. The application of this intersectional framework must be considered more seriously within the scientific community in order to transcend systems of oppression that lead to normative thought.

By understanding and taking ownership of foundational flaws in the way research is conducted, progress can be made to unpack systems-thinking towards a more interdisciplinary approach rooted in diverse thought. As a self-identified queer man, I recognize first-hand the systematic dehumanization that can thrive within the scientific community. The field of sexual

psychology may serve as a case study. Broadly, many researchers exclude sexual minorities for projects that do not explicitly investigate the lives of these sexual minorities in question. This suggests that the only epistemological value of these communities lies in their underrepresented status, and this provides an example of reinforcement that some individuals are too *other* to be considered for equal inclusion among "normal" participants (Anders, Goldey, & Bell, 2014).

The field of sexuality studies also relies on the use of antiquated measurement tools of identity that minimize the diverse experiences of queer individuals. The Kinsey scale is often used as a means to categorize and identify participants' sexual orientation (Figure 15). The main disadvantage of the Kinsey scale lies in how the questions lay rooted in gender. For individuals not interested in gender identity/expression as a factor in sexual attraction, such as the case for individuals identifying as pansexual, this scale becomes problematic. Furthermore, some individuals answering the Kinsey questions may be genderqueer or trans-identified themselves and/or attracted to genderqueer or trans-identified individuals (Anders, Goldey, & Bell, 2014), which increasingly complicates the use of the Kinsey scale. All in all, the fluidity of intense attractions may confound the usefulness of the scale. While an individual may possess no feelings of attraction towards a member of the same sex at one moment, this does not absolutely determine their attractions for the future, which are subject to change.

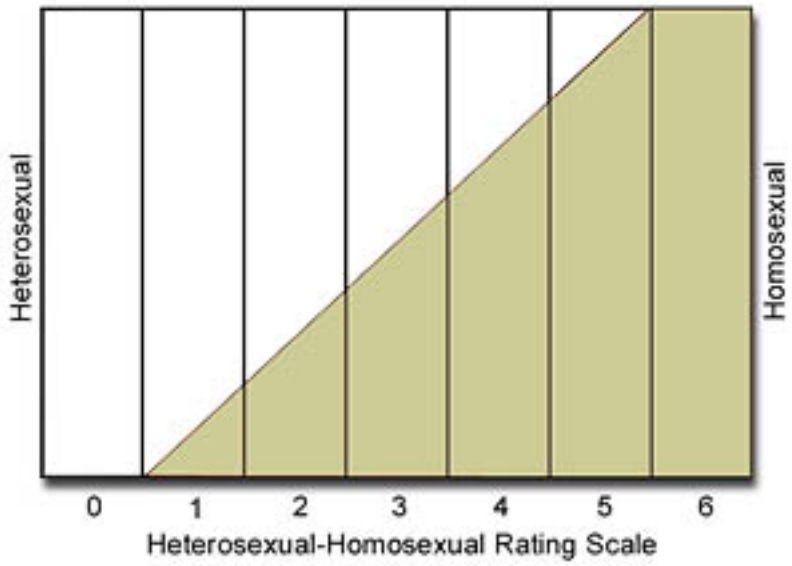

Figure 15. Kinsey Scale for Sexual Orientation. Categorization tool that includes questions of behavior, attraction, and/or fantasy on a scale of 0-6, ranging from exclusively gender/sex identities other than the subject to exclusively gender/sex identities the same as the subject (The Kinsey Institute, 2014).

As shown, the scientific community may be both implicitly and explicitly biased in the way it approaches etiological concerns: explicitly in the way that patients may be recruited and implicitly in the way that their orientations may be categorized and analyzed. Though it is seemingly unrelated subject matter relative to the developing retina of zebrafish, this case study serves as a powerful testament to the inherent value in diverse thought. The intersection of my scientist and queer identities allows me the opportunity to constructively critique the standardized methodologies used to investigate sexual minorities, an opportunity that may not be accessible to another scientist without the lived experiences that I hold. By placing more value on the social identities and intersectionalities of individuals within the scientific community, diverse thought can allow innovative techniques to tackling questions that seek to explore the workings of the natural world and prevent systematic ways of thinking.

My past two years of work within the Raymond Lab have been inspiring in a number of ways, and the lab serves as a prime example of a diverse environment that drives a productive,

supportive community of scientific inquiry. With individuals of varying gender, citizenship, race, sexual orientation, age, socioeconomic status, and interests, the lab microenvironment inherently values the diverse lived experiences of its members. This formation of a community that values diversity so deeply could not thrive, however, without the support of Dr. Pamela Raymond. When she first became Chair of the Department of Molecular, Cellular, & Developmental Biology in 2005, she was the only female full professor in the department, and she has since continued to work with U-M ADVANCE, a program that promotes diverse faulty hiring and retention (Plumhoff, 2014). As a champion for a variety of perspectives in science, Raymond creates an inclusive lab environment, which I have found incredibly empowering as an individual overtly conscious of the ways that power, privilege, and oppression have shaped my worldview.

When met with roadblocks and failures within my experimentation, Raymond met my frustration with seasoned words. She explained how scientific investigation represents a winding, never-ending trajectory. Stops along the way that seemingly inhibit progress, such as extraneous variables and unanticipated confounds, truly fuel a deeper understanding of the way the world works and posits a new multitude of fascinating questions that may have never been considered before. Science indeed breeds excellence. By engaging in conversations of social justice and diversity, the creation of supportive, heterogeneous communities facilitates a view of the natural world through a spectrum of lenses, which in turn enables a collective upheaval of conventional thinking that unlocks the potential for innovative and deliberate scientific exploration.

ACKNOWLEDGEMENTS:

Many thanks go to Dr. Pamela Raymond and Mikiko Nagashima for their guidance and support with my project. I'm also appreciative of Linda Barthel, Christopher Sifuentes, Jenny Chung, Alcides Gonzales, Dilip Pawar, and Komal Govil for their energy and enthusiasm in the lab. Lastly, thanks to the stars and back to my friends and family for their good vibes and encouragement throughout this process. The National Science Foundation and the MCDB Summer Research Award financially supported my work.

Works Cited

Allison, W., Barthel, L., Skebo, K., Takechi, M., Kawamura, S., & Raymond, P. (2010). Ontogeny of cone photoreceptor mosaics in zebrafish. *The Journal of Comparative Neurology, 518*, 4182-4195.

Anders, S. (2012). From One Bioscientist to Another: Guidelines for Researching and Writing About Bisexuality for the Lab and Biosciences. *Journal of Bisexuality,* 393-403.

Anders, S., Goldey, K., & Bell, S. (2014). Measurement of Testosterone in Human Sexuality Research: Methodological Considerations. *Archives of Sexual Behavior, 43*, 231-250.

Bernardos, B., Barthel L., Meyers, J., Raymond, P. (2007). Late-stage neuronal progenitors in the retina are radial müller glia that function as retinal stem cells. *The Journal of Neuroscience, 27*(26), 7028-7040.

Centanin, L., Hoeckendorf, B., & Wittbrodt, J. (2011). Fate restriction and multipotency in retinal stem cells. *Cell Stem Cell, 9*, 553-562.

Crenshaw, K. (1991). Mapping the margins: Intersectionality, identity politics, and violence against women of color. *Stanford Law Review*, *43*(6), 1241– 1299.

Curado, S., Anderson, R., Jungblut, B., Mumm, J., Schroeter, E., & Stainier, D. (2007). Conditional targeted cell ablation in zebrafish: A new tool for regeneration studies. *Developmental Dynamics, 236*, 1025-1035.

Francis, A., Smith, F., & Pfuderer, P. (1974). A heart-rate bioassay for crowding factors in goldfish. *The Progressive Fish-Culturist, 36*(4), 196-200.

Frantz, R. (2005). Swimming against the stream. Herbert Simon, Harvey Leibenstein, George Shackle, Friedrich von Hayek. In *Two minds: Intuition and analysis in the history of economic thought*. New York, N.Y.: Springer.

The Kinsey Institute for Research in Sex, Gender, and Reproduction. (2014). Retrieved from http://www.kinseyinstitute.org/

Pfuderer, P., Williams, P., & Francis, A. (1974). Partial purification of the crowding factor from Carassius auratus and Cyprinus carpio. *The Journal of Experimental Zoology, 187*(3), 375-382.

Plumhoff, K. (2014, January 27). Molecular, cellular, and developmental biology chair champions women in science. *The University Record*. Retrieved March 1, 2015, from http://record.umich.edu/articles/molecular-cellular-and-developmental-biology-chair-champions-women-science

Raymond, R. & Barthel, L. (2004). A moving wave patterns the cone photoreceptor mosaic array in the zebrafish retina. *International Journal of Developmental Biology, 48,* 935-945.

The Sense Organs. (1957). In M. Brown (Ed.), *The physiology of fishes* (Vol. 2). New York: Academic Press.

Walls, G. (1942). Higher Fishes. In *The vertebrate eye and its adaptive radiation* (pp. 573-588). Bloomfield Hills, MI: Cranbrook Institute of Science.

Win, Z., Barthel, L., & Raymond, P. (2009). Genetic evidence for shared mechanisms of epimorphic regeneration in zebrafish. *PNAS, 106*(23), 9310-9315.

Yoshikawa, S., Norcom, E., Nakamura, H., Yee, R., & Zhao, X. (2007). Transgenic analysis of the anterior eye-specific enhancers of the zebrafishgelsolin-like 1 (gsnl1) gene. *Developmental Dynamics, 236*, 1929-1938.

Yu, M., & Perlmutter, A. (1970). Growth inhibiting factors in the zebrafish, *Brachydanio rerio* and the blue guarami, *Trichogaster trichopterus*. *Growth, 34*, 153-175.